Eur. Phys. J. D **8**, 305–308 (2000)

THE EUROPEAN PHYSICAL JOURNAL D

EDP Sciences

Rapid Note

Unexpected reduction of the spin-exchange cross-section for fast $^3He^+$ ions incident on Rb atoms

Y. Arimoto[1,a], N. Shimakura[2,b], K. Yonehara[3,c], T. Yamagata[3,d], and M. Tanaka[4,e]

[1] Research Center for Nuclear Physics (RCNP), Osaka University, Mihogaoka 10-1, Ibaraki, Osaka 567-0047, Japan
[2] Department of Chemistry, Niigata University, Ikarashi Nino-cho 8050, Niigata 950-2181, Japan
[3] Department of Physics, Konan University, Okamoto 8-9-1, Higashinada-ku, Kobe 658-8501, Japan
[4] Kobe Tokiwa College, Ohtani-cho 2-6-2, Nagata-ku, Kobe 653-0838, Japan

Received 11 September 1999 and Received in final form 28 December 1999

Abstract. The spin-exchange cross-section, σ_{se}, was measured for a 6.33 keV/amu $^3He^+$ ion incident on a polarized Rb atom. The result is $\sigma_{se} = 0.12^{+0.27}_{-0.26} \times 10^{-15}$ cm^2, which is unexpectedly an order of magnitude smaller than the theoretical value $\sigma_{se} = 5.9 \times 10^{-15}$ cm^2 evaluated by the semiclassical impact parameter method assuming formation of a single molecular state.

PACS. 34.50.-s Scattering of atoms, molecules, and ions – 34.10.+x General theories and models of atomic and molecular collisions and interactions (including statistical theories, transition state, stochastic and trajectory models, etc.) – 31.15.Rh Valence bond calculations

Spin-exchange processes in atom-atom collisions have received much attention since Purcell and Field [1] explained the intensity of the 21-cm line radiation in radio astronomy by this mechanism. This process in atomic collisions is not only of fundamental importance in quantum mechanics but it is also of practical interest for various applications such as optical pumping [2], H masers [3], polarized ion sources [4], etc. It has been extensively studied in a low energy region (< a few eV) for the H–H [1,5–7], H–Rb [8,9], He–Rb [10,11], muonium-Cs [12] systems, etc. However, so far, the studies of spin-exchange processes at higher energies have been limited only to the H–Rb [4,13], He^+–Na [14] and Ne^+–N [15] systems.

One of the current topics is the spin-exchange process for the fast (> a few keV/amu) $^3He^+$–Rb system in view of application to the polarized ion source for nuclear physics research [16–18]. In this letter we report the first measurement of the spin-exchange cross-section, σ_{se}, for this system, using a polarized Rb vapor. We also report a theoretical calculation of σ_{se} by the semiclassical impact parameter method assuming formation of a single molecular state. This paper is a follow-up paper on reference [18].

[a] e-mail: arimoto@rcnp.osaka-u.ac.jp
[b] e-mail: shima@shimakura.sc.niigata-u.ac.jp
[c] e-mail: yonehara@rcnp.osaka-u.ac.jp
[d] e-mail: yamagata@center.konan-u.ac.jp
[e] e-mail: tanaka@rcnp.osaka-u.ac.jp

The spin-exchange cross-section is measured by observing the induced polarization of the $^3He^+$ ion after an unpolarized $^3He^+$ ion penetrates a polarized Rb vapor. Here, the Rb vapor thickness should be at least 1×10^{14} atoms/cm^2 to obtain a detectable polarization of the $^3He^+$ ion, since the magnitude of the spin-exchange cross-section is expected to be on the order of 10^{-15} cm^2 according to the theoretical estimation as discussed later. It should be noted that with such a thick vapor the $^3He^+$ ion is polarized not only by the spin-exchange process itself but also by multiple cycles of electron stripping and capture called "electron pumping" [16,18]. The polarization induced by the latter process is correctly evaluated since the electron stripping and capture cross-sections are well established [19,20]. Though the spin-exchange process between a ^3He atom formed in the electron pumping process and a Rb atom also produces the polarization, this effect is expected to be small as discussed later.

A schematic view of the experimental apparatus is shown in Figure 1. The $^3He^+$ ions were produced by a duoplasmatron ion source and were extracted at 19 kV. The $^3He^+$ ions were momentum analyzed by a sector magnet and led into a Rb oven which was located in the center of a 2T-superconducting solenoidal magnet. A Rb vapor inside the oven was polarized by means of the optical pumping with a high power (4 W) Ti:sapphire laser excited by a 25 W-Ar ion laser. The thickness and polarization of the Rb vapor were measured by the Faraday rotation method [21]. After passing through the

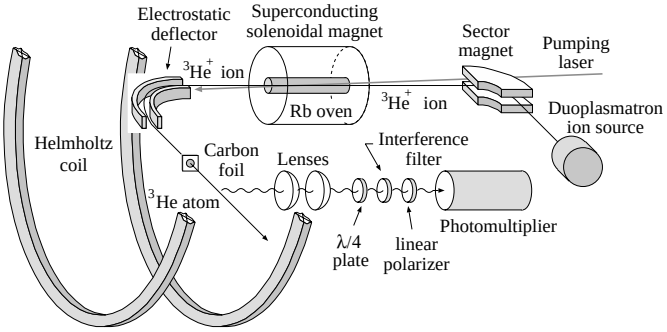

Fig. 1. A schematic view of the experimental apparatus.

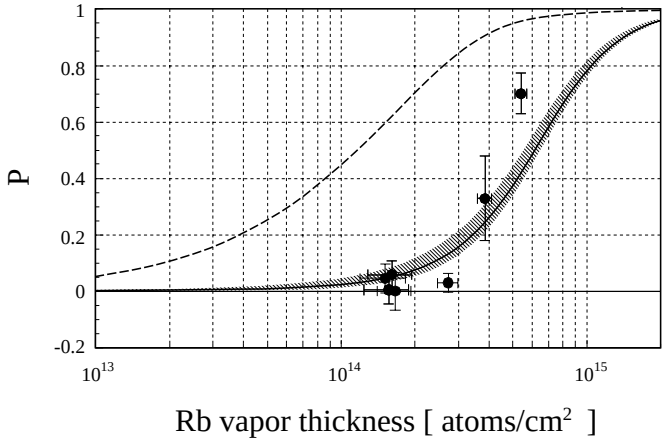

Fig. 2. Observed P (●) plotted as a function of the Rb vapor thickness. The solid curve shows the theoretical curve with σ_{se} obtained by the χ^2 fitting method. The shaded area corresponds to the errors of σ_{se}. The dashed curve is the theoretical curve assuming $\sigma_{se} = 5.9 \times 10^{-15}$ cm^2 which is calculated by the semiclassical impact parameter method.

region of the solenoidal magnetic field, the polarization is transferred from the $^3He^+$ ion to the ^3He nucleus by the hyperfine interaction. Then, the nuclear polarized $^3He^+$ ions were energy analyzed by an electrostatic deflector and were introduced into a polarimeter, with which the nuclear polarization was measured. To avoid depolarization by stray magnetic fields, a uniform magnetic field was applied to the region of the deflector and the polarimeter by a Helmholtz coil.

The principle of the polarimeter is based on beam-foil spectroscopy [22]. The nuclear polarized $^3He^+$ ion penetrating a 5 μg/cm^2 carbon foil captures an electron to become electrically neutral, while being populated in an excited state. The ^3He atom in flight deexcites to the ground or metastable states by emitting photons. During the photon emission a certain amount of the polarization is periodically transferred from the nucleus to the atom by the hyperfine interaction. Consequently, the nuclear polarization can be determined by measuring the circular polarization of the emitted photons. Photons at 388.9 nm corresponding to the transition between the 3^3P_J ($J = 0$, 1 or 2) and 2^3S_1 states were used in the present measurement. The photons were analyzed with polarization optics consisting of a $\lambda/4$ plate, an interference filter and a linear polarizer and finally detected by a photomultiplier. As a result, the polarization of the $^3He^+$ ions, P_I, was obtained from the measured ^3He nuclear polarization, P_N, assuming $P_I = 2P_N$. Here, P_N is expressed by

$$P_N = A^{-1}S/I, \tag{1}$$

where A = 0.207, and S/I is given by $S/I = \{I(\sigma^+) - I(\sigma^-)\}/\{I(\sigma^+) + I(\sigma^-)\}$ with $I(\sigma^+)$ and $I(\sigma^-)$ = intensity of the right- and left-handed circularly polarized photons at 388.9 nm [23].

A typical value of P_N was 7% at the Rb vapor thickness of 5.5×10^{14} atoms/cm^2. The $^3He^+$ ion current and photon counting rate were typically 150 nA and 5 kcps. Data accumulation time needed for each Rb vapor thickness was about 10 minutes. The Rb polarization decreased from 60% to 20% according to an increase of the Rb thickness from 2×10^{14} to 10×10^{15} atoms/cm^2.

For a detailed description of the experimental procedure the reader is referred to reference [18].

The polarization of the $^3He^+$ ions, P, thus obtained is plotted as a function of the Rb vapor thickness in Figure 2.

Here, P is the $^3He^+$ polarization normalized by the Rb polarization.

It is clearly seen that P increases according to an increase of the Rb vapor thickness. This behavior is qualitatively understood as follows: when the Rb vapor thickness is increased, the number of collision cycles between the ^3He ion/atom and Rb atoms is increased. The polarization of the $^3He^+$ ions increase cumulatively as the result of the spin-exchange and the electron pumping processes [18].

To discuss the above behavior quantitatively, we solved rate equations, in which the above processes were taken into account. For this purpose the prescription given in the preceding work [16] has been modified. The rate equations were expressed in terms of matrices as shown below

$$\frac{\mathrm{d}}{\mathrm{d}\pi}\mathbf{F} = (\epsilon_+\mathsf{R}_+ + \epsilon_-\mathsf{R}_-)\mathbf{F}, \tag{2}$$

where π is the Rb vapor thickness and ϵ_+ and ϵ_- are

$$\epsilon_+ = \frac{1 + P_{Rb}}{2}, \quad \epsilon_- = \frac{1 - P_{Rb}}{2}, \tag{3}$$

where P_{Rb} is the Rb polarization. Here $\mathbf{F}$ and $\mathsf{R}_\pm$ are given in equations (4–6)

$$\mathbf{F} = \begin{pmatrix} H^+_{1/2} \\ H^+_{-1/2} \\ H_{t1} \\ H_{t0} \\ H_{t-1} \\ H_{s0} \end{pmatrix}, \tag{4}$$

$$\mathsf{R}_+ = \begin{pmatrix} -\sigma_{10} & \sigma_{\rm se} & \sigma_{\rm t1} & \frac{\sigma_{\rm t1}}{2} & 0 & \frac{\sigma_{\rm s1}}{2} \\ 0 & -\sigma_{10}-\sigma_{\rm se} & 0 & \frac{\sigma_{\rm t1}}{2} & \sigma_{\rm t1} & \frac{\sigma_{\rm s1}}{2} \\ \sigma_{10} & 0 & -\sigma_{\rm t1} & \sigma_{\rm sea} & 0 & 0 \\ 0 & \frac{\sigma_{10}}{2} & 0 & -\sigma_{\rm t1}-\sigma_{\rm sea} & \sigma_{\rm sea} & 0 \\ 0 & 0 & 0 & 0 & -\sigma_{\rm t1}-\sigma_{\rm sea} & 0 \\ 0 & \frac{\sigma_{10}}{2} & 0 & 0 & 0 & -\sigma_{\rm s1} \end{pmatrix}, \quad (5)$$

$$\mathsf{R}_- = \mathsf{T}\mathsf{R}_+\mathsf{T}^{-1}, \quad \mathsf{T} = \begin{pmatrix} 0&1&0&0&0&0 \\ 1&0&0&0&0&0 \\ 0&0&0&0&1&0 \\ 0&0&0&1&0&0 \\ 0&0&1&0&0&0 \\ 0&0&0&0&0&1 \end{pmatrix}. \quad (6)$$

H_j^+ is the population of $^3He^+$ ions in the $m_z = j$ states. H_{tJ} is the population of triplet ^{3}He atoms in the $m_z = J$ states, and H_{s0} is the population of singlet ^{3}He atoms. σ_{ij} is the cross-section from state i to state j where $i = 1$ is for a $^3He^+$ ion, $i =$ t(s) is for a triplet(singlet) ^{3}He atom, $j = 0$ is for a ^{3}He atom and $j = 1$ is for a $^3He^+$ ion. $\sigma_{\rm se}$ is the spin-exchange cross-section for $^3He^+$ ions and $\sigma_{\rm sea}$ is that for ^{3}He atoms. In this calculation we used the capture and stripping cross-sections $\sigma_{10} = 4.18\pm0.30\times10^{-15}$ cm^2, $\sigma_{\rm t1} = 1.08\pm0.32\times10^{-15}$ cm^2, $\sigma_{\rm s1} = 0.012\times10^{-15}$ cm^2 taken from the results of experiments on the He–Rb [19] and He–Cs [20] systems. The only unknown parameters are $\sigma_{\rm se}$ for $^3He^+$ ions and $\sigma_{\rm sea}$ for ^{3}He atoms. However, $\sigma_{\rm sea}$ does not significantly influence the value of P for the following intuitive reason: since the ^{3}He atom is formed by the polarized electron capture in the cycle of electron pumping, the atom is highly polarized. As a result, a further growth of the atomic polarization by the spin-exchange becomes less pronounced. In other words, $\sigma_{\rm sea}$ is not as influential as $\sigma_{\rm se}$. Indeed, the insensitivity of P on $\sigma_{\rm sea}$ was ensured by the calculation of P with various $\sigma_{\rm sea}$. Thus, the discussion below is done only for $\sigma_{\rm se}$ assuming that $\sigma_{\rm sea}$ is fixed at 1.0×10^{-15} cm^2 for convenience.

Under the above assumptions, the experimental results were fitted by parameterizing $\sigma_{\rm se}$ with the χ^2 fitting method. In the present χ^2 fitting, we employed errors combined by experimental errors of polarization, σ_P, and of Rb vapor thickness, σ_π, as expressed by

$$\sigma = \sqrt{\sigma_P^2 + \left(\mathrm{d}P/\mathrm{d}\pi\right)^2 \sigma_\pi^2}. \quad (7)$$

The most probable value of $\sigma_{\rm se}$ was derived from the minimum value of χ^2, $\chi^2_{\rm min}(= 20.5)$, and the error of $\sigma_{\rm se}$ was obtained by the deviation of $\sigma_{\rm se}$ when the value of χ^2 was $\chi^2_{\rm min}\pm\chi^2_{\rm min}/(n-1)$, where n is the number of data points. To include the effect of the errors in the capture and stripping cross-sections, the shifts in $\sigma_{\rm se}$ were evaluated when the capture and stripping cross-sections were varied by their errors.

The best fitted curve is shown by a solid curve in Figure 2. The spin-exchange cross-section is

$$\sigma_{\rm se} = 0.12\,^{+0.27}_{-0.26}\times10^{-15}\ \mathrm{cm}^2. \quad (8)$$

The shaded area in Figure 2 corresponds to the errors in equation (8). From this analysis, it is found that the observed P was well reproduced by the model calculation including the processes of the spin-exchange and the electron pumping.

Since it is of particular interest to see whether the experimental spin-exchange cross-section, $\sigma_{\rm se}$, is reproduced by the theory or not, we carried out a calculation by the semiclassical impact parameter method assuming formation of a single molecular state. This procedure succeeded in reproducing the experimental results for the fast H–Rb system [4,13].

In this formalism, the $\sigma_{\rm se}$ is given as [13],

$$\sigma_{\rm se} = 2\pi\int_0^\infty b\sin^2\frac{\phi_{\rm ts}}{2}\,\mathrm{d}b, \quad (9)$$

$$\phi_{\rm ts} = \int\frac{V_{\rm t}-V_{\rm s}}{\hbar}\,\mathrm{d}t = -2\int_b^\infty\frac{R(V_{\rm t}-V_{\rm s})}{\hbar v\sqrt{R^2-b^2}}\,\mathrm{d}R. \quad (10)$$

Here, $V_{\rm t}$ and $V_{\rm s}$ are respectively the potential energies of the $(^3$He–Rb$)^+$ molecule in the $1^3\Sigma$ and $1^1\Sigma$ (1Σ denotes $^3He^+(1s^1)$–Rb$(5s)$) states. b, R and v are respectively impact parameter, internuclear separation between the Rb atom and the $^3He^+$ ion, and incident velocity of the $^3He^+$ ion.

In order to determine the energy difference between $V_{\rm t}$ and $V_{\rm s}$, *i.e.* $V_{\rm ts}$, the molecular electronic states for the $^3He^+$–Rb system were calculated by using the valence-bond configuration-interaction method with the Gaussian type pseudopotentials representing the Rb^+ core [24]. The pseudopotential parameters for the Rb^+ core and the Slater type orbitals (STO's) for the Rb atom were taken from reference [24]. We obtained the orbital exponents of the STO's for the He atom by optimizing its energies. The experimental spectroscopic energies at the separated atom limit are reproduced to better than 0.04% except for the lowest state, ^{3}He$(1s^2\ 1S)$–Rb^+ (0.8%), in the present calculation. Figure 3 shows the present results of $V_{\rm ts}$ for $^3He^+$–Rb along with the result for the H–Rb system of reference [24], as solid and dot-dashed curves, respectively.

The $\sigma_{\rm se}$ was calculated as a function of incident energy of the $^3He^+$ ion by substituting the $V_{\rm ts}$ for the $^3He^+$–Rb system into equation (10). This result is shown by a solid curve in Figure 4. The experimental data at 6.33 keV/amu is also shown by a closed circle. For comparison, the results for the H–Rb system are also shown in Figure 4, where the dot-dashed curve is the theoretical result [13] and open circles are the experimental results [4]. The calculation predicts that $\sigma_{\rm se}$ for the $^3He^+$–Rb system is several times larger than that for the H–Rb system at all studied energies. The trend is qualitatively understood from Figure 3, in terms of the difference in the shape of $V_{\rm ts}$ between these

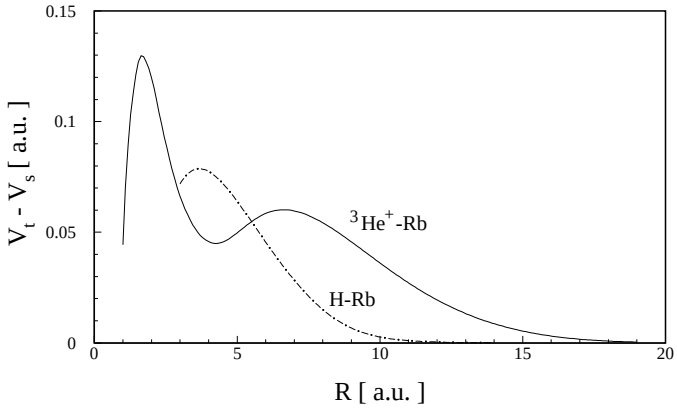

Fig. 3. Potential energy difference, V_{ts}, between the $1^1\Sigma$ and $1^3\Sigma$ states plotted as a function of the internuclear separation. The solid curve is the result of the present calculation for the $^3He^+$–Rb system and the dot-dashed curve is the result of the calculation for the H–Rb system by Stevens *et al.* [24].

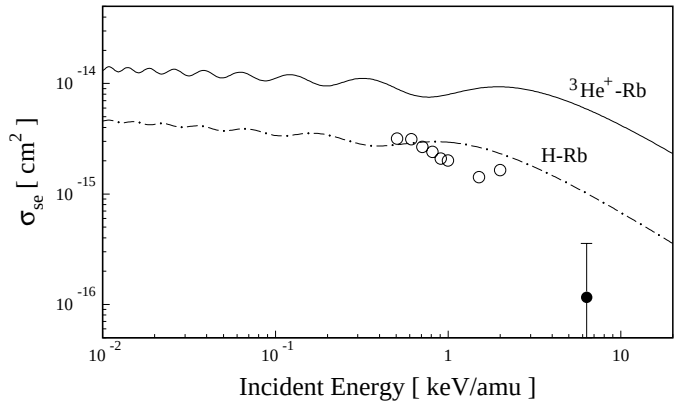

Fig. 4. σ_{se} calculated as a function of the incident energy for a H atom (the dot-dashed curve) [13] and a $^3He^+$ ion (the solid curve) incident on a Rb atom and experimental σ_{se} for the H atom (○) [4] and the $^3He^+$ ion (●).

two systems, *i.e.*, σ_{se} becomes larger for the $^3He^+$–Rb than for the H–Rb, because V_{ts} extends to larger R in the case of $^3He^+$–Rb system.

A striking result is that the experimental value of σ_{se} for the $^3He^+$–Rb system is an order of magnitude smaller than the theoretical prediction, while those for the H–Rb system are reasonably reproduced by the theory.

Referring back to Figure 2, the polarization dependence on Rb vapor thickness is shown for the theoretical value, $\sigma_{se} = 5.9\times10^{-15}$ cm^2. As expected, the polarization is overestimated.

The unexpected reduction of σ_{se} for the $^3He^+$–Rb system has not been known so far because no experimental data have been available due to experimental difficulty. This suggests that the collision mechanism for the $^3He^+$–Rb system is much more complex than that for the H–Rb system. In fact, we assumed only one transition channel for both systems. However, it may be necessary to take the effect of other transition channels into account, particularly for the $^3He^+$–Rb system. A more comprehensive calculation along this line is now under way.

This work was supported by the Research Center for Nuclear Physics (RCNP) Osaka University. The authors wish to express their sincere appreciation to the RCNP ex-director, Prof. H. Ejiri and director, Prof. Y. Nagai for their encouragement and support throughout this work. The authors also thank Prof. Rangacharyulu for critically reading the manuscript.

References

1. E.M. Purcell, G.B. Field, Astrophys. J. **124**, 542 (1956).
2. T.G. Walker, W. Happer, Rev. Mod. Phys. **69**, 629 (1997).
3. S.B. Crampton, H.G. Robinson, D. Kleppner, N. Ramsey, Phys. Rev. **141**, 55 (1966).
4. A.N. Zelenski *et al.*, AIP Conf. Proc. **339**, 650 (1995), in *8th International Symposium on Polarization Phenomena in Nuclear Physics (SPIN 94)*.
5. J.P. Wittke, R.H. Dicke, Phys. Rev. **103**, 620 (1956).
6. M.E. Hayden, M.D. Hürlimann, W.N. Hardy, Phys. Rev. A **53**, 1589 (1996).
7. A. Dalgarno, M.R. Rudge, Proc. R. Soc. Lond. A **286**, 519 (1965).
8. S.G. Redsun, R.J. Knize, G.D. Cates, W. Happer, Phys. Rev. A **42**, 1293 (1990).
9. H.R. Cole, R.E. Olson, Phys. Rev. A **31**, 2137 (1985).
10. K.P. Coulter, Ph.D. thesis, Princeton University, 1989.
11. T.G. Walker, Phys. Rev. A **40**, 4959 (1989).
12. J.J. Pan *et al.*, Phys. Rev. A **48**, 1218 (1993).
13. D.R. Swenson, D. Tupa, L.W. Anderson, J. Phys. B **18**, 4433 (1985).
14. W. Jitschin *et al.*, Phys. Rev. A **34**, 3684 (1986).
15. S. Osimitsch *et al.*, Phys. Rev. A **40**, 2958 (1989).
16. M. Tanaka, M. Fujiwara, S. Nakayama, L.W. Anderson, Phys. Rev. A **52**, 392 (1995).
17. T. Yamagata *et al.*, Nucl. Instrum. Meth. A **402**, 199 (1998).
18. M. Tanaka *et al.*, Phys. Rev. A **60**, R3354 (1999).
19. R.J. Girnius, L.W. Anderson, Nucl. Instrum. Meth. **137**, 373 (1976).
20. A.S. Schlachter, D.H. Loyd, P.J. Bjorkholm, L.W. Anderson, W. Haeberli, Phys. Rev. **174**, 201 (1968).
21. F. Strumia, Nuovo Cimento B **44**, 378 (1966).
22. H.J. Andrä, Phys. Scripta **9**, 257 (1974).
23. T. Ohshima *et al.*, Phys. Lett. B **274**, 163 (1992).
24. W.J. Stevens, A.M. Karo, J.R. Hiskes, J. Chem. Phys. **74**, 3989 (1981).